International Atomic Energy Agency

INDC(CCP)-355
Distr. G

INDC INTERNATIONAL NUCLEAR DATA COMMITTEE

INELASTIC SCATTERING OF 1-2.5 MeV NEUTRONS BY ^{235}U AND ^{238}U NUCLEI

N.V. Kornilov, A.B. Kagalenko, V.Ya. Baryba,
A.V. Balitskij, A.A. Androsenko, P.A. Androsenko

Power Physics Institute
Obninsk, Russia

1991

IAEA NUCLEAR DATA SECTION, WAGRAMERSTRASSE 5, A-1400 VIENNA

INDC(CCP)-355
Distr. G

INELASTIC SCATTERING OF 1-2.5 MeV NEUTRONS BY ^{235}U AND ^{238}U NUCLEI

N.V. Kornilov, A.B. Kagalenko, V.Ya. Baryba,
A.V. Balitskij, A.A. Androsenko, P.A. Androsenko

Power Physics Institute
Obninsk, Russia

1991

Printed by the IAEA in Austria
July 1993

93-02787

ABSTRACT

The inelastic scattering cross-sections of 1-2.5 MeV neutrons for ^{235}U and ^{238}U nuclei were measured. A detailed description is given of the data processing procedures used, and the methods for determining the neutron flux in the sample. The Monte Carlo method was used to calculate the corrections for multiple neutron scattering and neutron flux attenuation in the sample. Pursuant to an analysis of the fission neutron spectra, we concluded that the systematic error level of the results is $\pm$ 3.2%. The results of these cross-section and spectrum measurements for inelastically scattered neutrons are compared with results from other sources and existing evaluations, the possible causes of the divergences for neutrons with an energy level of less than 1 MeV are analysed, and suggestions are put forward for future research work.

Introduction

Measurements of the differential cross-sections for neutron inelastic scattering by fissile nuclei in the MeV range are needed principally to satisfy the practical requirements of the nuclear power industry, and these requirements are far from being satisfied. In a number of cases, the results of the latest experiments [1] and the evaluated data differ by as much as 30-50%. In the new evaluations for ^{235}U [2], the inelastic scattering cross-section is ~ 1.5 times higher than the value given in the ENDF/B-5 library, and this needs to be further substantiated.

Study of the inelastic scattering cross-sections for fissile nuclei involves a number of methodological problems. Because of the high density of low-lying states the scattering cross-sections cannot be measured reliably at the individual levels and the contribution of elastic scattering cannot be separated. Moreover, the finite recording threshold imposes a lower limit of 200-500 keV on the measured neutron spectra. For these reasons, it is difficult to measure the total inelastic scattering cross-sections and to compare the results from various sources. These problems were largely solved in Ref. [1],

which measured the "pseudo-elastic" scattering cross-section for a number of fissile nuclei. In the latter study it was concluded that the inelastic scattering cross-sections for ^{233}U, ^{235}U, ^{238}U and ^{232}Th were known to within reasonable accuracy, that they agreed satisfactorily with the ENDF/B-5 evaluation, and that the energy distribution of scattered neutrons for these nuclei needed further refinement.

The above has helped determine the aim of this work, which is to study neutron inelastic scattering with a view to refining the total inelastic scattering cross-section and scattered neutron spectra. In order to achieve this end, we paid special attention to lowering of the recording threshold, improvement of measurement accuracy, experimental modelling, and consideration of the contribution of non-monoenergetic source neutrons.

1. Experimental method

The spectra of inelastically scattered neutrons were measured by the time-of-flight method with the spectrometer of the EhG-1 accelerator at the Power Physics Institute. The main parameters of the spectrometer were as follows: pulse length ~ 1 ns; pulse repetion frequency 2 MHz; path length ~ 2 m; average current at target 4-6 μA. In order to generate neutrons, we used the T(p,n) reaction in a solid tritium-scandium target 0.2 mg/cm^2 thick. The neutron spectrometer is described in detail in Ref. [3]. Below we give only the main parameters of the present experiment.

Samples of metallic ^{235}U and ^{238}U in the form of a disk 10 mm thick and 46.3 mm in diameter were placed at a distance of 9.5 cm from the neutron source. The normal to the sample surface lay in the "source-sample-detector" plane and was turned in relation to the incident proton direction through an angle (-30°). The percentage content of the samples was 99.5% for the

^{238}U sample, and 89.6% ^{235}U and 10.4% ^{238}U for the ^{235}U sample. The samples were packaged in an Al container with a wall thickness of 0.3 mm.

The neutron detector was a plastic scintillator 80 mm in diameter and 20 mm thick placed in a massive collimator. The end surface of the detector was coated with a layer of lead 2 mm thick to reduce the gamma background. The detector efficiency (recording threshold ~ 100 keV) was measured in relation to the ^{252}Cf fission neutron spectrum, for which purpose, the ^{252}Cf source was positioned in the same place as the sample to be investigated. The neutron spectrum shape was calculated from the data of Ref. [11] in the following form:

$$S(E) = f(E) \cdot M(E),$$

where M(E) is the Maxwell distribution with T = 1.42 MeV. Function f(E) was represented in the form of a power series with the coefficients:

$a_0 = 0.95411$, $a_1 = 4.680014-2$, $a_2 = -9.28259-3$, $a_3 = -2.633332-4$,

$a_4 = 1.30966-4$, $a_5 = -8.40658-6$, $a_6 = 1.662338-7$.

All the scattered neutron spectra were measured at an angle of 120°. Each spectrum was produced from 10-12 measurements lasting approximately one hour.

For each initial neutron energy, we performed a minimum of two scattered neutron spectrum measurements with the sample.

In addition, we measured:

- the neutron spectra with the Al container;
- the neutron spectra with a carbon sample;
- the source neutron spectra at an angle of 0°.

2. Data processing

In the first processing stage, the quality of the accelerator operation was checked for each measurement (time resolution and energy stability) using

the measured spectra from the time-of-flight monitor. The spectra of the "good" measurements were summed. Uncorrelated background was subtracted from the summed spectra. The spectrum of the main detector was measured in the form of a two-dimensional time•amplitude data set (512•32). Thus, for each amplitude interval the time region where the effect did not occur was known. When subtracting the steady background, this region was assumed to be zero. This processing algorithm improved the measurement accuracy in the low-energy scattered neutron region. The time shift for the whole amplitude range did not exceed ~ 0.5 ns (one channel being equal to 1 ns), and it was not taken into account when the two-dimensional distribution was converted into a one-dimensional time data set.

The resultant time spectrum was normalized to the readings of the "long" counter, and the background spectrum measured with the Al container was subtracted from it. Figure 1 shows the time distributions for the experiment with the sample (effect plus background) and the Al container (background), which were obtained at this stage of the processing after subtraction of the uncorrelated background for ^{238}U, for an initial neutron energy of 1.17 MeV.

The time spectrum was converted to an energy scale and normalized to obtain the absolute cross-sections; a correction was introduced for the recording efficiency; the contribution of scattering by ^{238}U was subtracted for the ^{235}U sample. The "non-monoenergetic" neutron background, determined from "direct" flux measurements was also subtracted. Here we assumed that there was only elastic scattering, and this is justified in view of the low value of this background (3-5%).

3. Determination of the neutron flux on the sample

The neutron flux on the sample was measured in two ways.

1. Relative to elastic scattering by carbon

Here, the sample under investigation was replaced by a carbon sample (diameter 51 mm, thickness 15 mm). The measured values of $S_x(E)$ and S_c are related to the cross-sections for the sample under investigation $\sigma_x(E)$ and for carbon σ_c by the following expressions:

$$S_x(E) = \sigma_x(E)\ \Phi_x\ N_x\ \Omega\ \varepsilon(E)\ \alpha_x(E), \tag{1}$$

$$S_c = \sigma_c\ \Phi_c\ N_c\ \Omega\ \varepsilon(E_c)\ \alpha_c, \tag{2}$$

$$\sigma_x(E) = k_c \frac{S_x(E)}{\varepsilon(E)\ \alpha_x(E)} \tag{3}$$

$$k_c = \sigma_c \frac{1}{S_C} \frac{N_c}{N_x} \frac{\Phi_c}{\Phi_x}\ \varepsilon(E_c)\ \alpha_c\ , \tag{4}$$

where Φ is the neutron fluence, N the number of nuclei in the sample, Ω the solid angle of the detector, $\varepsilon(E)$ the scattered neutron recording efficiency, and $\alpha(E)$ the correction for attenuation and multiple scattering. The subscripts x and c stand for the sample under investigation and carbon; k_c is the normalizing constant for this method of determining the neutron flux.

The spectrum of the neutrons scattered by carbon is shown in Fig. 2. As may be seen from Fig. 2, the model calculation satisfactorily describes the

distribution shape. The plateau in the low-energy region is due to the process of multiple scattering. Because multiply scattered neutrons leave the elastic peak region, α_c depends on the region of integration. In order to reduce the uncertainty associated with the consideration of non-monoenergetic neutrons from the source, we tried to make the spectrum integration limits as close as possible when obtaining the values S_c and α_c. These limits coincided with the limits of the elastic peak which was calculated without the contribution of multiple scattering.

2. Relative to the fission of ^{235}U

Here, we used the readings from a fission chamber positioned between the neutron source and the sample. The diameter of the layer was 30 mm, the thickness on each side of the aluminium substrate was t = 0.54 mg/cm^2, and the total weight of ^{235}U was 7.5 mg. In this case, the following functions must also be used in addition to expressions (1) and (3):

$$S_f = \sigma_f \Phi_f N_f \varepsilon_1 \varepsilon_2 \varepsilon_3 \qquad (5)$$

$$k_f = \sigma_f \frac{1}{S_f} \frac{N_f}{N_x} \frac{\Phi_f}{\Phi_x} \frac{1}{\Omega} \varepsilon_1 \varepsilon_2 \varepsilon_3 , \qquad (6)$$

where S_f is the total number of fission fragments above the discrimination threshold, ε_1,ε_2 are the proportion of the fragments lost in the layer and under the discrimination threshold, and ε_3 is the contribution of "thermal" neutrons.

The values of ε_2 and ε_3 were determined experimentally, and ε_1 was calculated by the following formula:

$$\varepsilon_1 = 1 - t/2R, \qquad (7)$$

where R is the mean fragment range in the U_3O_8 layer. In the calculations it was assumed that R = 10 mg/cm^2, which yielded $\varepsilon_1 = 0.97$. Losses under the recording threshold were determined by extrapolating the fragment spectrum from the plateau region to zero amplitude, $\varepsilon_2 = 0.989$.

To determine ε_3, we measured the dependence of the fission chamber count rate on the distance. Figure 3 shows experimental data for various functional dependences $\Phi_f(r)$. As can be seen from Fig. 4, the experimental data are described by a linear dependence on $x = \eta(r)\ \ln(1 + r_o^2/r^2)$, where η is the factor which takes account of the angular distribution of the neutrons from the source, r_o is the radius of the layer, and r is the distance from the source to the layer. The method of least squares was used to determine the coefficients of the equation:

$$\Phi(x)=a_o+ a_1\ x \qquad (8)$$

and $\varepsilon_3 = (1 + a_o/a_1\ x_1)$, where x_1 is the value of x for the working position of the fission chamber. The proportion of "thermal" neutrons is virtually independent of energy and amounts to (4.8 $\pm$ 0.5%).

The neutron flux on the sample was calculated as a function of the energy by the Monte Carlo method, taking into account the kinematics of the T(p,n) reaction and energy loss in the active layer of the target. The calculation parameters - target thickness and incident particle energy spread - were determined by comparing the calculated neutron distributions for the T(p,n) and Sc(p,n) reactions with experiment [3]. In these calculations, the ratios Φ_f/Φ_x and Φ_c/Φ_x were also determined. As we can see from expression (4) and (6), k_c and k_f are practically independent of each other. There is

some correlation which is due only to the determination of the neutron flux ratio.

Table 1 gives the errors of determination of k_c and k_f. The errors of the reference cross-sections are taken from Ref. [5]. For the total scattering cross-section for carbon this report gives an error of 0.53%, which seems excessively optimistic. The scattering cross-section for carbon at an angle of 120° is taken from Ref. [5] and the fission cross-section of ^{235}U from ENDF/B-6. We applied both normalization methods to every measurement. The value of k_c is systematically higher than k_f by 2.8% for the carbon measurements, by 4.5% for ^{238}U and by 5.4% for ^{235}U. The cause of this difference is unclear although, as Table 1 shows, these values do not exceed the estimated accuracy of their determination. Subsequently we used the average values $k = (k_f + k_c)/2$ for normalization. The actual accuracy of the experiment will be analysed below.

4. Multiple scattering and attenuation of the neutron flux

The Monte Carlo method and the BRAND program package [4] were used to calculate the corrections for multiple scattering and attenuation of neutrons both in the samples under investigation and in carbon. As may be seen from Fig. 2, a satisfactory description of the shape of the single scattering was obtained. Thus, the modelling of the neutron source would seem to be fairly accurate. The systematic difference between the experimental and calculated distributions in the low-energy region appears to be associated with the "non-monoenergetic" neutron background.

Figures 4 and 5 show the secondary neutron spectra (scattering and fission) together with the calculation results. It should be noted that the calculation does not just describe the neutron interaction process in the

sample but fully models the experiment from the source to the detector. Two calculations were carried out for each energy and sample. In one, the interaction process in the sample was modelled in full, and in the other only the geometrical factors and the time and energy spreads were retained. The correction was determined as the ratio of these values. The calculation was carried out using a time scale. The results were converted into energy distributions using the experimental spectra processing program.

For the calculation we used neutron data from the NEDAM library [8]. As we may see from Figs 4 and 5, this set of neutron data does not describe the experiment. The correction for multiple scattering and attenuation determined from these calculations may significantly distort the experimental results in certain cases, especially for ^{238}U. Therefore, when determining the inelastic scattering cross-section the correction was made for the integral values in the case of which the shape of the scattered neutron spectra has a less substantial influence. When analysing the smooth spectra (fission neutron spectrum and inelastic scattering spectrum for ^{235}U), the correction was made in the energy distributions. Table 2 gives the corrections for multiple scattering and attenuation α_x and α_c.

5. Fission neutron spectra

In the experiment we measured only part of the fission neutron spectrum in a fairly narrow energy range ~ 2-6 MeV, and we therefore did not attempt to study in detail the shape of the fission neutron spectrum.

The angular distribution of fission neutrons for initial energies of ~ 2 MeV is isotropic or symmetrical relative to 90° with a weak angular dependence [9], so that our data only have to be multiplied by 4π to obtain values integrated with respect to the angle. The number of secondary neutrons

ν and the fission cross-sections σ_f for ^{235}U and ^{238}U are known to an accuracy of 1-2%. We can therefore determine the accuracy of the experiment by comparing the experimental values of $(\nu\sigma_f)$ with the evaluated values. Various dependences were used to describe the spectrum shape: the Maxwellian distribution with parameters taken from Ref. [6] and our experimental data (Table 3); the Watt distribution with parameters taken from ENDF/B-5 (^{235}U) and ENDF/B-6 (^{238}U); and the Madland-Nix distribution (ENDF/B-6) for ^{235}U.

When using the Maxwellian distribution with any set of parameters the experimental values of $(\nu\sigma_f)$ are ~10% higher than the evaluated values. A description of the neutron spectrum using the Watt formula substantially improves the agreement. This is due to the fact that for close average neutron energies the Watt distribution reduces the proportion of neutrons with an energy of < 1 MeV (Fig. 6).

Figure 7 gives the ratios of the experimental and evaluated values of $(\nu\sigma_f)$ and here all the data - the average number of prompt fission neutrons, the fission cross-sections and the spectra - are taken from ENDF/B-6. The data spread is 2.2%, and the data for ^{235}U are systematically shifted by 2.2%. The quadratic combination of these values - 3.2% - can be used as an estimate to determine the systematic measurement error for the integral values in the present experiment. This value includes the errors of normalization and determination of the detector efficiency, and the corrections for multiple scattering and attenuation. When determining the error of the inelastic scattering cross-section below, the statistical error for each measurement has been added to this value.

6. Neutron inelastic scattering cross-sections

Table 4 gives the integral inelastic scattering cross-sections. The first column gives the initial neutron energy on the sample and its root mean square deviation; the second column gives the integration limits. The fourth column gives the experimental cross-sections - including part of the fission neutron spectrum - corrected for multiple scattering and attenuation effects. The fifth column gives the cross-sections, after subtraction of the fission neutron contribution, multiplied by 4π. The sixth and seventh columns give the scattering cross-sections at levels which were not covered by the region of integration in ENDF/B-6, and the total inelastic scattering cross-sections.

The errors in the table were determined from the systematic experimental error estimated above and the statistical accuracy of the integral values. Let us analyse the factors which affect the inelastic scattering cross-sections (fifth column of Table 4) but are not included in the experimental error.

1. In integrating the experimental spectra we used linear interpolation between the first point of the spectrum (150-180 keV) and 0 at E = 0. For ^{235}U, the scattered neutron spectra are described by the Maxwellian distribution with parameter T ~ 0.4 MeV. The use of this dependence increases the cross-section by ~ 50 mb.

2. The uncertainty associated with the subtraction of the fission neutrons can be evaluated by comparing the proportion of the fission neutron spectrum covered by the region of integration according to the ENDF/B-5 and ENDF/B-6 data. For ^{235}U, ENDF/B-6 gives values which are 3.3%, 2.9% and 1.3% lower

for the initial energies of 1.17, 1.79 and 2.19 MeV, respectively. This changes the inelastic scattering cross-section by ~30 mb and ~10 mb for ^{238}U.

3. When determining the systematic experimental error, we concluded that a number of factors, including the correction for multiple scattering, were known to an accuracy of at least 3.2%. This conclusion is valid only for the hard part of the spectra > 2 MeV.

4. The cross-section integrated with respect to the angles was obtained on the assumption that the angular distribution of inelastically scattered neutrons was described by the second Legendre polynomial. The uncertainty associated with this assumption is difficult to determine unambiguously, but this feature of our work should be taken into account.

7. Discussion of results

Figure 8 gives the total inelastic scattering cross-sections according to our data and the data of other studies, together with the evaluated cross-sections from various libraries. Of course, the total "experimental" cross-sections given in the figures have been correlated to some extent with the data from the libraries since, when they were obtained, a notable proportion of the scattering cross-section at low-lying levels - which were taken from the same data banks - was added. However, this is necessary for a correct comparison of the results from the various studies.

For ^{238}U, the set of levels not included in the experimental cross-sections is more definite. In this study and in Ref. [1] it is the first one or two levels, the predominate contribution coming from the first. In the case of these levels, the difference between the evaluations of Ref. [10] and ENDF/B-6 is negligible; the total inelastic scattering cross-sections obtained in the present study and in Ref. [1], which show a

satisfactory agreement, are systematically higher than the evaluation given in Ref. [2] thus confirming the ENDF/B-6 data.

For ^{235}U, the set of levels which were not taken into account in the experiment is less definite. However, since the scattering cross-sections at the individual levels are small, this does not generate substantial errors. The data of the present study agree, within the limits of error, with those of Ref. [1] and the evaluation given in ENDF/B-6. The evaluations given in ENDF/B-5 and the other sources are based on the experimental points to which the scattering cross-section at low-lying levels has not been added. In the 1-2 MeV energy region, our data and the data from Ref. [1] do not confirm the cross-section behaviour suggested in Ref. [2].

The good agreement with the results in Ref. [1] demonstrates that, at present, both the total inelastic scattering cross-section and the scattered neutron spectra in the 1-3 MeV energy region are known to a fairly high level of reliability.

As we can see from Fig. 8, for ^{235}U in the < 1 MeV energy region there is a systematic difference between the results in Ref. [1] and the evaluated dependences. A similar difference may be observed for other odd nuclei as well. An analysis of the inelastically scattered neutron spectra reveals a possible cause for this lack of agreement.

Figure 9 shows the scattered neutron spectra for ^{235}U for various initial energies. The excitation energy of the residual U nucleus was calculated by expression (9):

$$E_n = \frac{E_o}{(A+1)^2}\left[\mu+\left(A^2-1+\mu^2-\frac{U}{E_o}A(A+1)\right)^{1/2}\right]^2 \qquad (9)$$

where E_o, E_n are the energies of the incident and scattered neutrons, μ is the cosine of the scattering angle, and A the mass number of the target nucleus. An interesting characteristic is observed at an initial energy of 1.17 MeV - there starts a fairly intensive process of scattering by the group of levels associated with the excitation of the rotational bands for $U > 0.6$ MeV.

Using nuclear level-density formalism, we can represent the scattered neutron spectrum in the form:

$$S(E_n) \sim E_n \rho(U), \tag{10}$$

where $\rho(U)$ is the nuclear level density at excitation energy U. From expression (10) we can calculate the inceasing sum of levels:

$$N(U) = \int_{0.2}^{U} \frac{S(E_n)}{E_n} dU \tag{11}$$

and compare it with the dependence $N_1(U)$ obtained from the low-lying level count. For comparison, we renormalize dependence (11) to $N_1(U)$ at the 0.6 MeV point in the following way:

$$N_r(U) = N_1(0.2) + N(U) \frac{N_1(0.6)-N_1(0.2)}{N(0.6)}. \tag{12}$$

Figure 10 shows the dependences $N_r(U)$ and $N_1(U)$ for ^{235}U at an initial energy of 1.17 MeV. The good agreement between the energy dependences is striking, as is the characteristic feature at ~ 0.6 MeV. Above this

energy there is a sharp rise in the level density and, consequently, we can expect changes in the shape of the energy dependence for the inelastic scattering cross-section. A similar effect occurs for ^{238}U but in a more striking form.

In evaluating the cross-sections, this characteristic was apparently not taken into account. The number of separate levels included in the calculation is insufficient to include the excitation energy ~ 0.6 MeV, and the use of the statistical approach involves difficulties with regard to the description of the level density at low excitation energies. The systematic divergence between the results in Ref. [1] and the evaluated data in the < 1 MeV energy region might be related to this effect. However, both the cross-sections and the spectra of neutron inelastic scattering must be studied further before any definitive conclusion may be drawn.

The authors would like to thank Mr. V.G. Pronyaev for useful discussions.

REFERENCES

[1] SMITH, A.B., GUENTHER, P.T., McKNIGHT, R.D., Nuclear Data for Science and Technology, Proc. of Intern. Conf. Antwerp, (1982).

[2] KLEPATSKIJ, A.V., KON'SHIN, V.A., et al., in: Problems of Atomic Science and Technology for Nuclear Constants, No. 3 (1987) 3 [in Russian].

[3] KORNILOV, N.V., KAGALENKO, A.B., et al., Preprint: FEhI-2174 (1991) [in RUssian].

[4] ANDROSENKO, A.A., ANDROSENKO, P.A., et al., in: Problems on Nuclear Science and Technology, Ser. Physics and Technology of Nuclear Reactors No. 7 (1985) 33 [in Russian].

[5] Nuclear Data Standards for Nuclear Measurements, IAEA Technical Report 227, Vienna (1983).

[6] KORNILOV, N.V., BARYBA, V.Ya., SAL'NIKOV, O.A., Proc. 5th All-Union Conference on Neutron Physics, Kiev (1980) [in Russian].

[7] BABA, M., WAKABAYASHI, H., et al., Journal of Nucl. Science and Tech., 27 7 (1990) 601.

[8] ADROSENKO, P.A., in: Problems of Atomic Science and Technology, Ser. Physics and Technology of Nuclear Reactors, No. 7 (1985) 45 [in Russian].

[9] BARYBA, V.Ya., ZHURAVLEV, B.V., KORNILOV, N.V., SAL'NIKOV, O.A., At. Ehnerg., 43 4 (1977) 266.

[10] ABAGYAN, L.P., BAZAZYANTS, N.O., NIKOLAEV, M.N., TSIBULYA, A.M., Group Constants for Reactor and Shielding Calculations, Ehnergoatomizdat (1981) [in Russian].

[11] MANCHART. W., Report IAEA-TECDOC-410, Vienna (1986) 158.

Table 1. Partial errors of normalization

Quantity	$\delta k_o/k_o$, %	$\delta k_r/k_r$, %
Φ_1/Φ_x	~2	~4
σ	<1	~2.5
N	<0.5	~2
c	<2	-
Corrections	~2	<2
Total error	~3.6	~5.5

Table 2. Corrections for multiple scattering and attenuation

Energy	^{235}U	^{238}U	^{12}C
1.17	1.244	1.295	0.850
1.79	1.230	1.131	0.893
2.19	1.190	1.083	0.916

Table 3. Parameters of the Maxwellian distribution

Energy	^{235}U		^{238}U	
	[6]	Present work	[6]	Present work
1.17	1.293	1.29 ± 0.05	1.290	
1.79	1.303	1.39 ± 0.07	1.298	1.34 ± 0.08
2.19	1.310	1.36 ± 0.06	1.305	1.31 ± 0.09

Table 4. Inelastic scattering cross-sections

E_o, MeV	E_1-E_2, MeV	nucl.	σ_{exp}, mb/sr	$\sigma_{in\ exp}$, b	σ_{lev}, b	$\sigma_{in\ tot}$, b
1.17	0-1.04	^{235}U	184.3 ± 10	1.39 ± 0.13	0.520	1.91
0.012	0-0.94	^{238}U	105.9 ± 10	1.30 ± 0.13	1.263	2.56
1.79	0-1.55	^{235}U	251.5 ± 9.6	1.64 ± 0.12	0.569	2.21
0.014	0-1.55	^{238}U	227.3 ± 9.3	2.27 ± 0.12	0.784	3.06
2.19	0-1.95	^{235}U	300.3 ± 11	1.84 ± 0.13	0.526	2.36
0.015	0-1.95	^{238}U	254.8 ± 10	2.39 ± 0.12	0.580	2.97

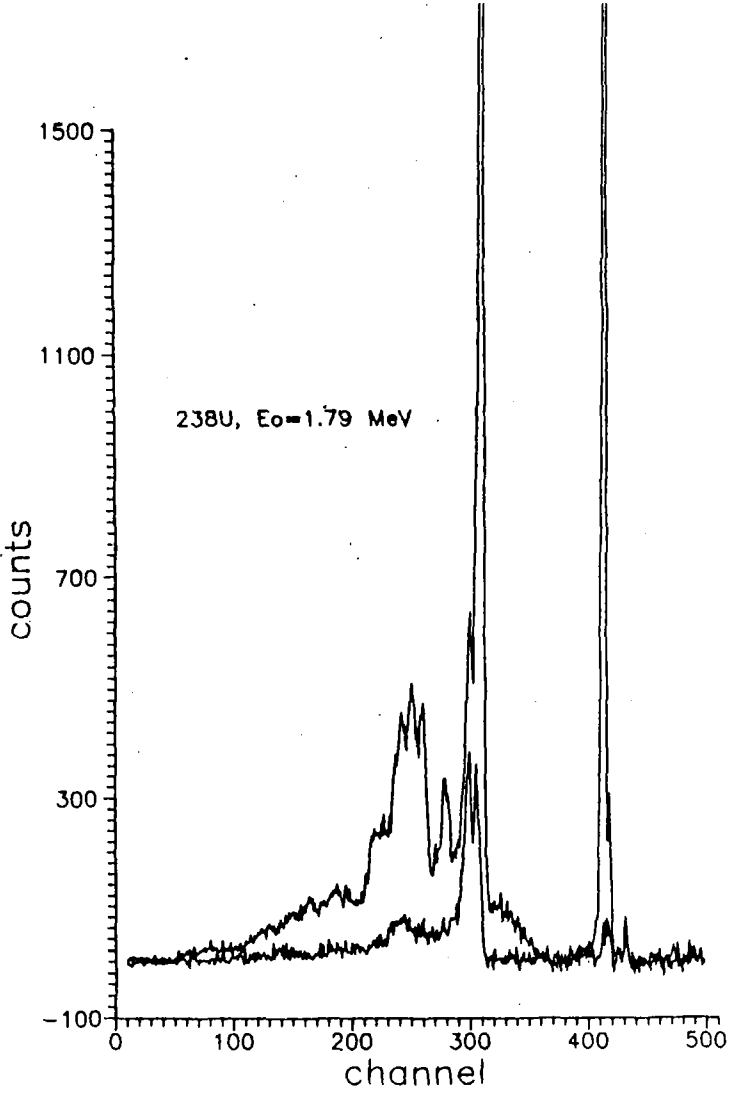

Fig. 1. Time spectrum of ^{238}U for an initial neutron energy of 1.17 MeV.

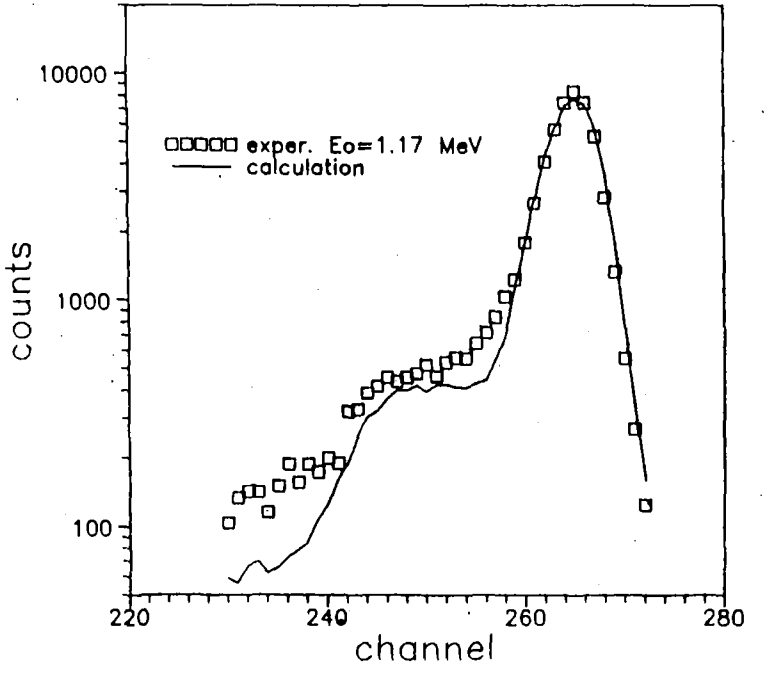

Fig. 2. Time spectrum of neutrons elastically scattered by carbon.

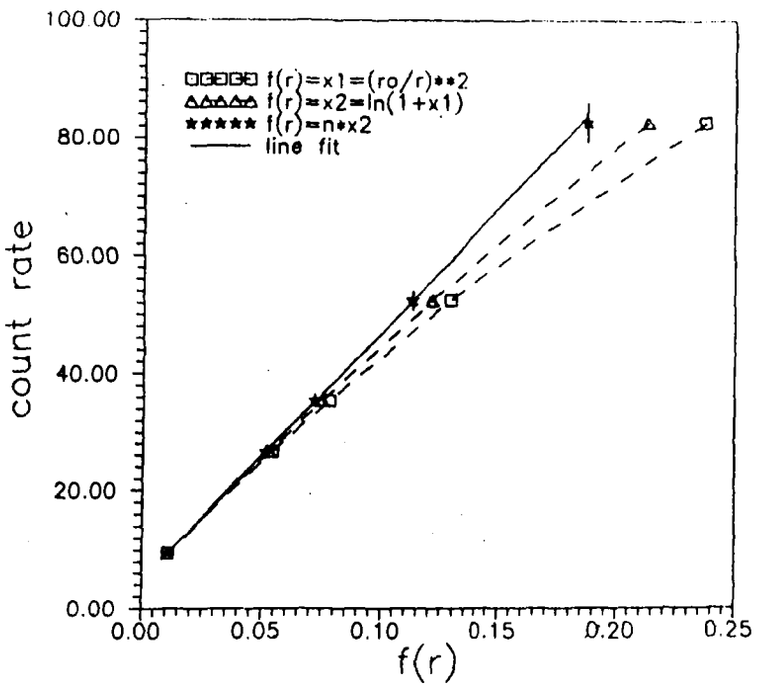

Fig. 3. Experimental data on the dependence of the neutron flux on the distance, in order to determine the proportion of "thermal" neutron fissions.

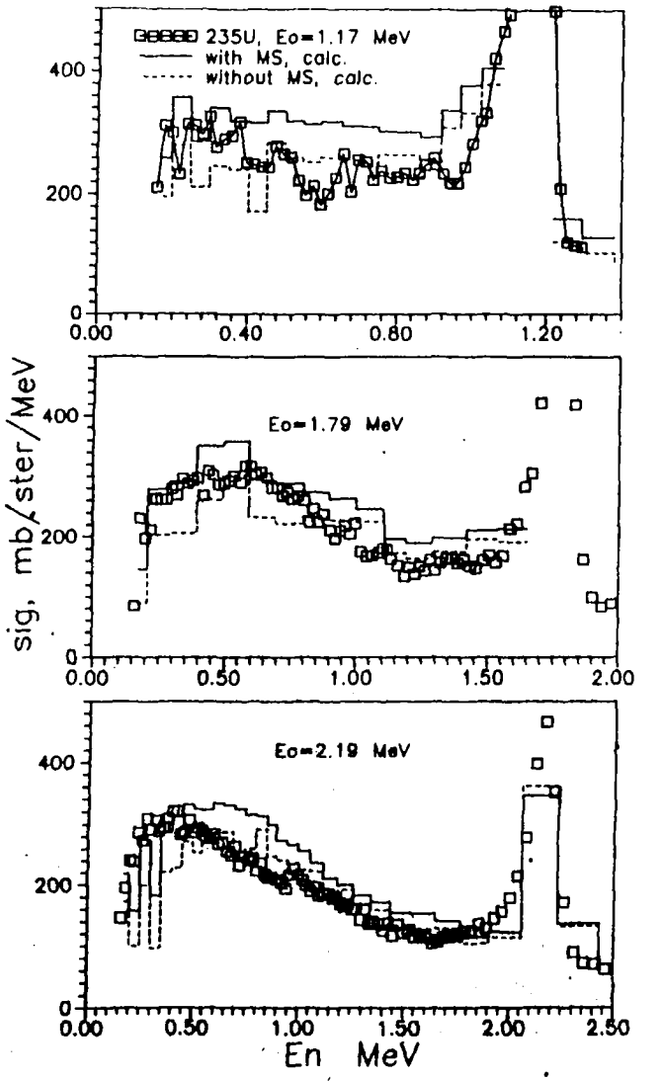

Fig. 4. Scattered neutron and fission neutron spectra for ^{235}U. The histograms show the results of calculation with (solid line) and without (dotted line) consideration of attenuation and multiple scattering.

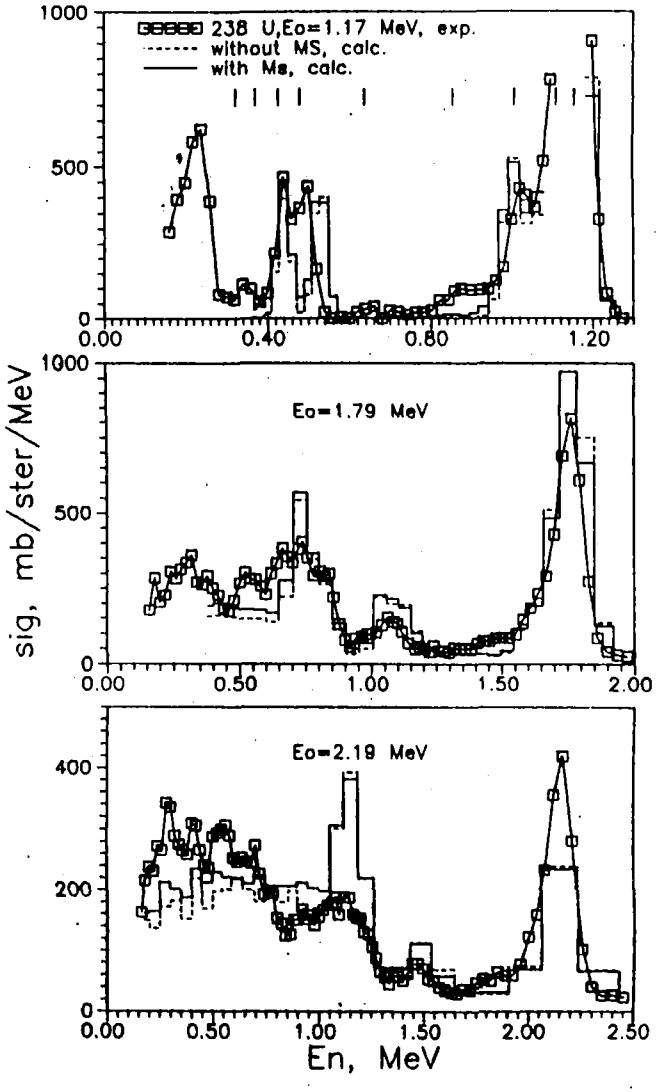

Fig. 5. Scattered neutron and fission neutron spectra for ^{238}U. The histograms show the results of calculation with (solid line) and without (dotted line) consideration of attenuation and multiple scattering.

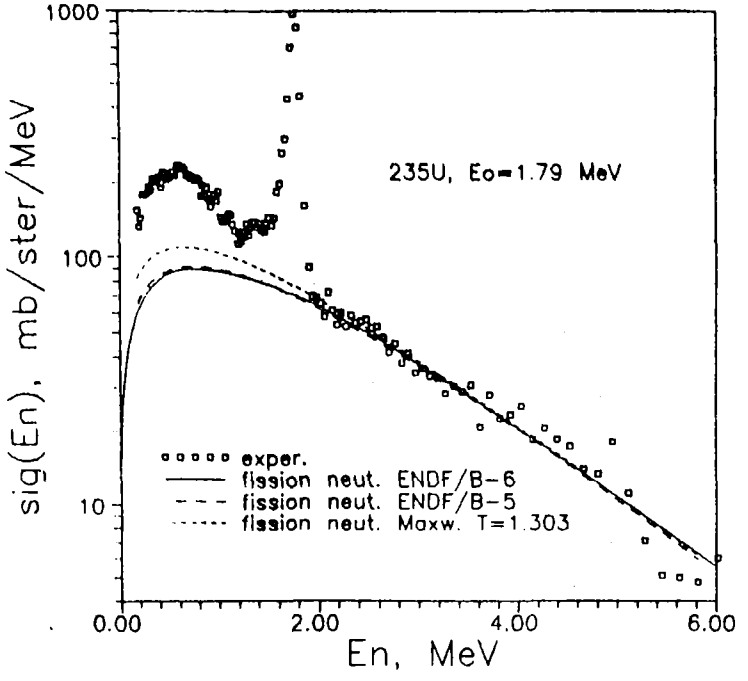

Fig. 6. Scattered neutron and fission neutron spectra for ^{235}U for an initial energy of 1.79 MeV. The lines show fission neutron spectra from various systematics normalized to the experiment.

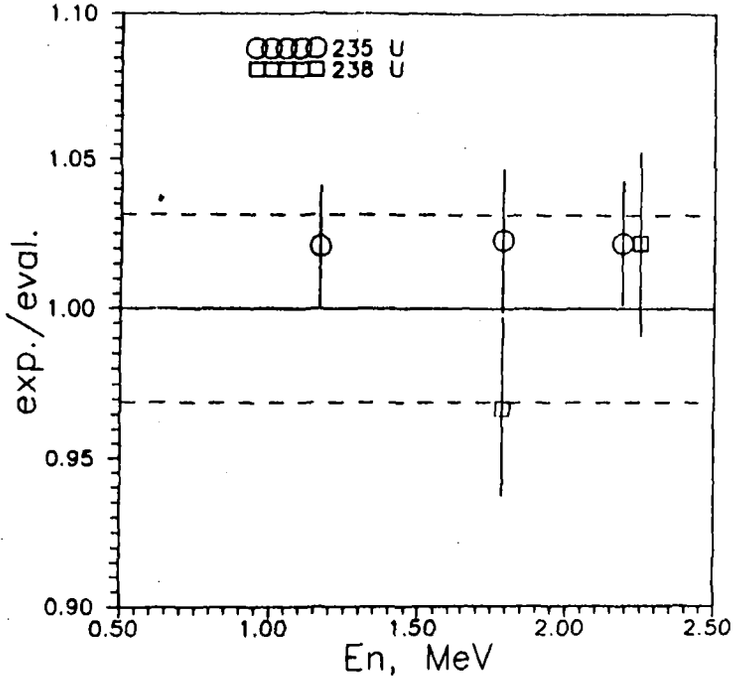

Fig. 7. Relationship of the experimental values of $(\nu\sigma_f)$ and the calculated values from ENDF/B-6. The errors for the points represent errors in the determination of the normalization coefficient for the fission spectrum. They are determined mainly by statistical accuracy. The dashed line shows the evaluated systematic experimental error of ± 3.2%.

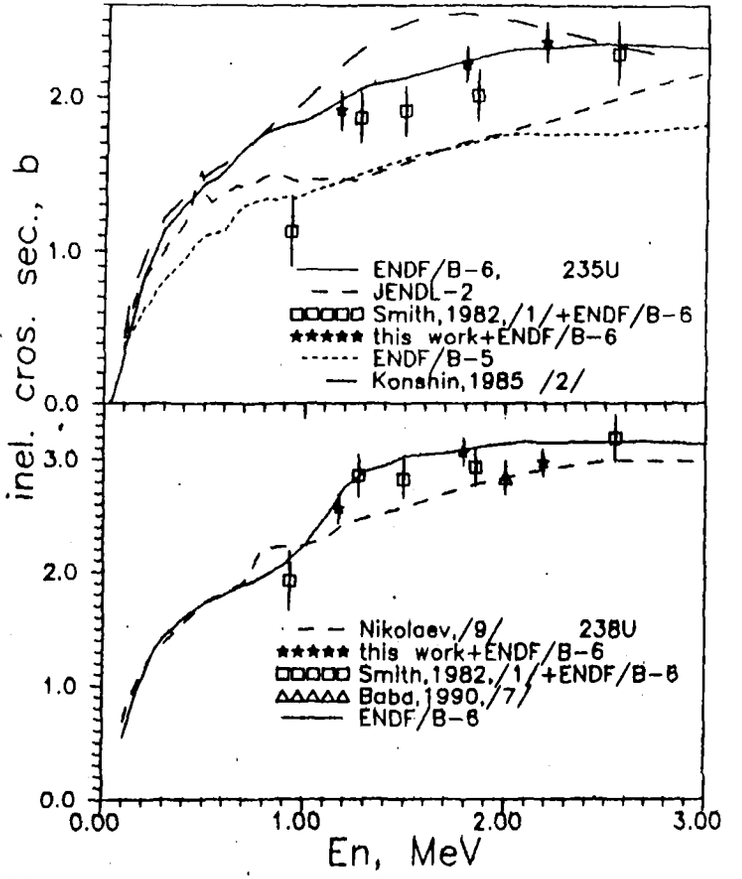

Fig. 8. Neutron inelastic scattering cross-sections for ^{235}U and ^{238}U nuclei.

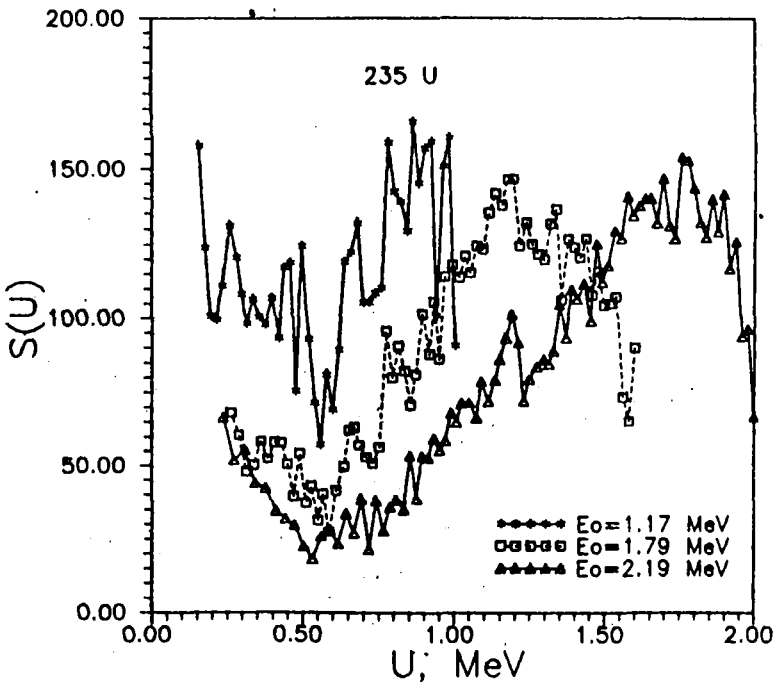

Fig. 9. Inelastically scattered neutron spectra for ^{235}U.

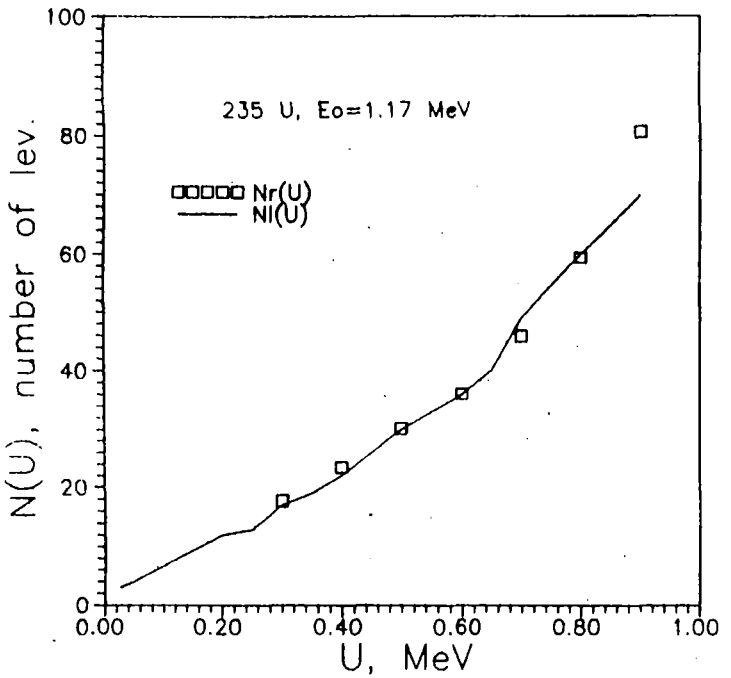

Fig. 10. Increasing sum of levels for ^{235}U.